Electronic Supplementary Material (ESI) for RSC Advances.

Detection of streptavidin-biotin intermediate metastable states at single-molecule level using high-temporal resolution atomic force microscopy

Evan Angelo Quimada Mondarte[a], Tatsuhiro Maekawa[a], Takashi Nyu[a], Hiroyuki Tahara[a], Ganchimeg Lkhamsuren[a], and Tomohiro Hayashi[*a,b]

[a]*Tokyo Institute of Technology, Department of Materials Science and Engineering, School of Materials and Chemical Technology (4259 Nagatsuta-cho, Midori-ku, Yokohama, Kanagawa 226-8503, JAPAN)*

[b]*JST-PRESTO (4-1-8 Hon-cho, Kawaguchi, Saitama 332-0012, JAPAN)*

[*]Corresponding author: hayashi.t.al@m.titech.ac.jp

Preparation of substrates and AFM probes

Preparation of substrates and AFM probes

Silicon substrates were treated in UV-Ozone (UV-300, SUMCO, Tokyo, Japan) for 15 minutes then were soaked to Piranha solution [sulfuric acid (H_2SO_4):30% hydrogen peroxide (H_2O_2)] in 3:1 v/v ratio for another 15 minutes to remove organic contaminants. After immersion, substrates were then rinsed with ethanol then dried using nitrogen gas flow.

The cleaned substrates were then subjected to metal deposition via thermal evaporation under vacuum (base pressure of 1.0×10^{-4} Pa). The substrates were set to the deposition stage maintained at 300°C overnight. A germanium (Ge) layer was first deposited for better stability and affinity of the gold metal to the substrates, resulting in a smooth Au surface. A 3-nm Ge film was deposited at a deposition rate of 0.1 Å/s followed by the deposition of Au film with 50 nm thickness at a deposition rate of 1 Å/s.

AFM probe cleaning

The probes used in this study are Olympus BL-AC40TS-C2 (BioLever mini). This type of probe has a silicon apex and a lever made of silicon nitride with a nominal spring constant of 90 pN/nm.

The probes were subjected to a UV-Ozone cleaner (UV-300, SUMCO, Tokyo, Japan) for a 15-min treatment to remove organic contaminants and hydroxylate the tip surface for further necessary functionalization. Next, the probes were immersed in a 0.1 M hydrochloric acid (HCl) to remove metallic contaminants for another 15 minutes before they were rinsed with ethanol for three times and then pure water (18.2 MΩ, Millipore, USA) for another three times.

Calculation of the effective spring constant (k_{eff})

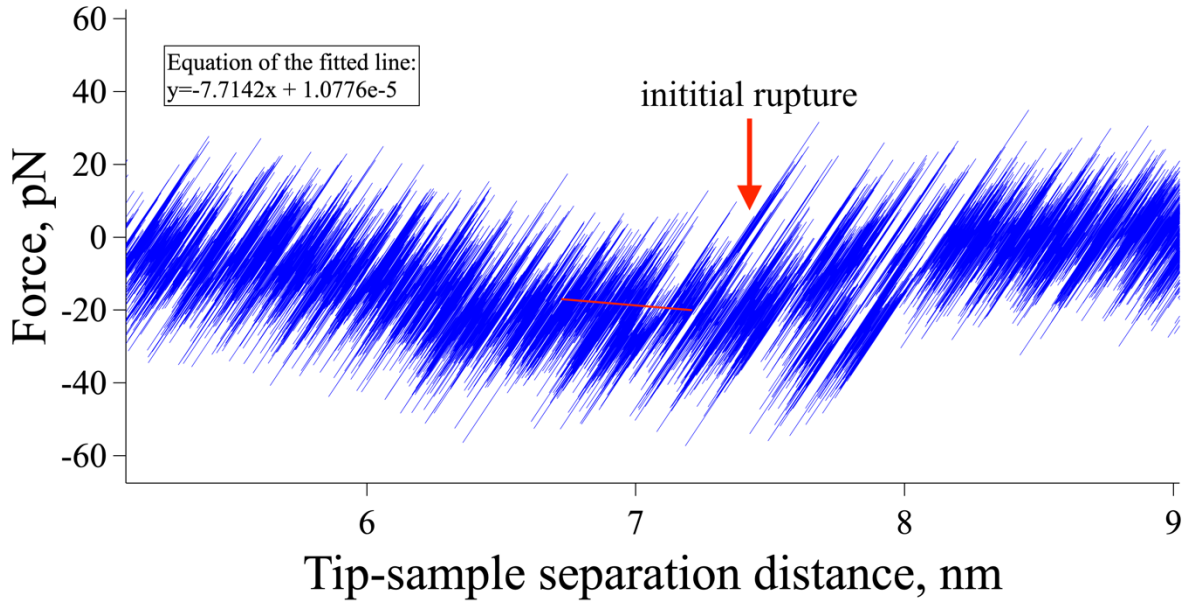

The slope of the fitted line at the region just before the occurrence of the first rupture of the force vs. separation distance plot gives an estimation of the linker spring constant at the vicinity of the detected streptavidin-biotin near-equilibrium force dynamics.

Plugging in the linker spring constant (k_l = 7.7 pN/nm), and the cantilever spring constant (k_c = 110.71 pN/nm) which was determined using the thermal noise method to equation 5, the effective spring constant (k_{eff}) is determined to be 7.2 pN/nm.

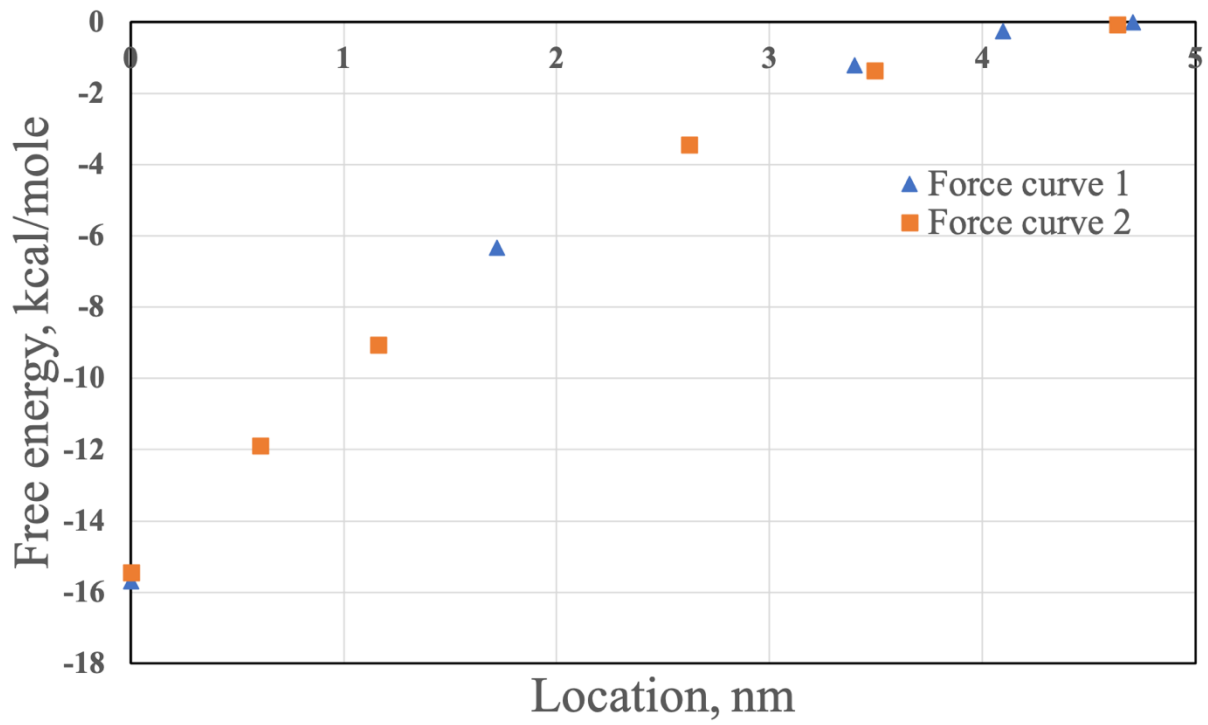

Fig. S1 $V(\Delta x)$ vs. location along the pulling reaction coordinate of the streptavidin-biotin system generated using two other force curves from the data set. In these measurements, the same loading rate and sampling rate presented in the methodology part were employed, and the calculated spring constants were 8.7 pN/nm and 9.9 pN/nm for force curves 1 and 2, respectively. Locations of the intermediate metastable states (given by the square and triangular markers) are in agreement with the energy landscape presented in Figure 6. In this case, each of the force-time curve does not contain the eight intermediate states presented in the main manuscript. However, when coupling with another force-time curve that detected another set of states, an energy landscape is obtained analogous to that in Figure 6. Moreover, it should also be noted that only the $V(\Delta x)$ values were obtained using the two force curves due to the fact that these force curves, unlike the one presented in the main manuscript, do not contain enough data to sample all states and transition events for the determination of lifetimes and the calculation of $\Delta G_{0,f}$ (see equations 1-3).

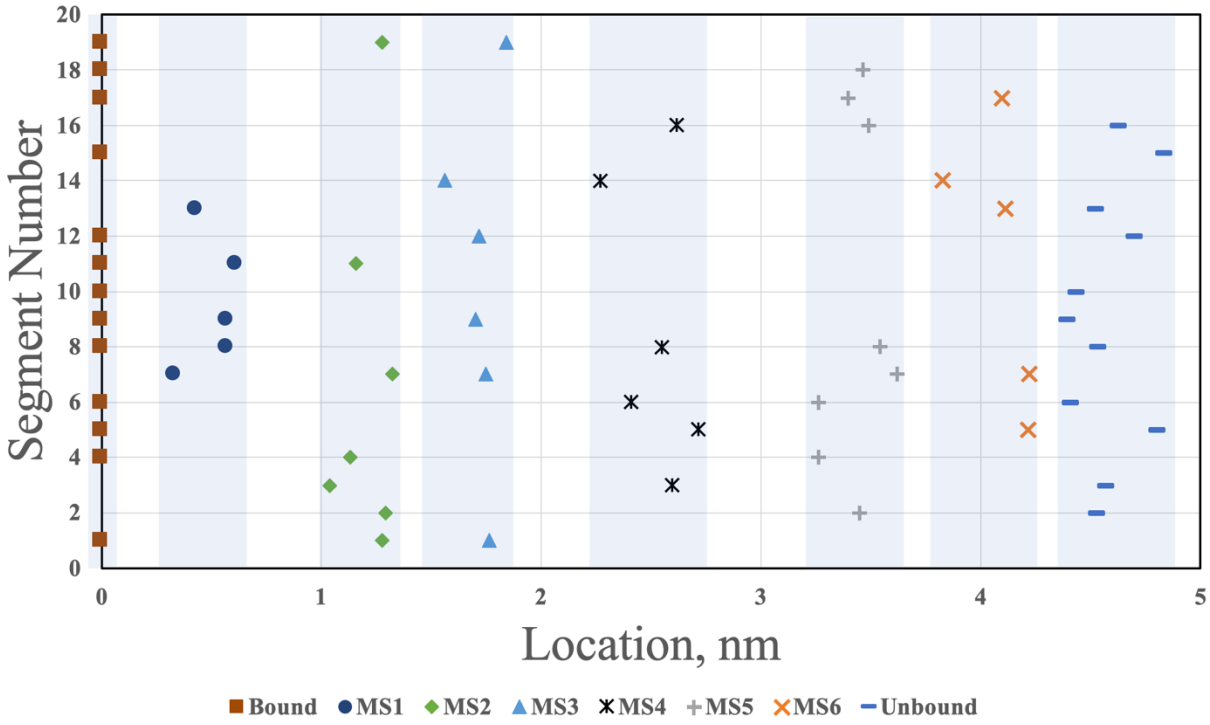

Fig. S2 Collection of all detected states from the data set of segmented force-time curves.